



Cite this: *Polym. Chem.*, 2019, **10**, 4920

Received 28th May 2019,  
Accepted 30th July 2019

DOI: 10.1039/c9py00780f

rsc.li/polymers

## Amino-diol borate complexation for controlling transport phenomena of penetrant molecules into polymeric matrices†

Matthew G. Unthank,<sup>a</sup> Colin Cameron,<sup>b</sup> Anthony Wright,<sup>b</sup> David Hughes,<sup>c</sup> M. Ashraf Alam<sup>c</sup> and Michael R. Probert<sup>d</sup>

The development of new high performance materials, coatings, composites and adhesives relies on insight into the origin of material performance on a molecular level. This paper explores a new type of epoxy-amine-borate (EAB) hybrid material for control of penetrant solvent molecules into cross-linked thermoset polymer networks.

### Introduction

Coatings, composites and adhesives made from epoxy resins are of huge commercial importance supplying a market predicted to be worth over \$14.26 billion by 2024.<sup>1</sup> Within the research field of epoxy thermoset polymers, the development of methods to control and prevent ingress of small molecules through these materials is critical in the development of new, more durable, high performance materials. Advances in this field can positively impact a wide range of important industrial applications across the aerospace, electronics, coatings, composites and adhesives industries. In these industries, preventing the transport of small molecules (including gasses) through polymer networks is of crucial importance. Controlling the uptake of compounds such as water, solvents, oils and environmental pollutants into polymeric materials is essential in maintaining their bulk properties such as mechanical and cohesive strength, interfacial adhesion, surface properties (such as gloss and texture) as well as material permeability. Important industrial examples include maintaining

the integrity of engineering and structural composites and plastics,<sup>2</sup> minimising gas transport through packaging, films and membranes<sup>3</sup> and controlling solvent molecule ingress into the coatings of chemical storage and transport tanks.<sup>4</sup> Within the marine shipping industry, the risk of cross-contamination of cargoes through retention of small molecules in organic coatings also presents a significant material challenge, particularly in the development of chemical resistant coatings for steel transport containers. In such containers, a diverse range of chemical cargoes are routinely transported sequentially in the same cargo tanks, leading to a cross-contamination risk. Thermoset coatings used in these applications are therefore optimised for solvent and fluid resistance through careful material selection and cure conditions to control the polymer network structure at a molecular level. This industry, in particular, is challenged with the development of improved chemical resistant coatings to achieve improved broad-spectrum chemical resistance across a wide range of penetrant molecules or cargoes.<sup>5,6</sup> Within this field, epoxy-amine coatings are the dominant technology with a track record spanning many decades. Whilst a significant body of both historical<sup>6</sup> and recent<sup>7–10</sup> research underpins this hugely important area of chemistry, truly innovative and relevant new materials based on epoxy-amine technology are still rare treasures in the modern coatings literature.

The absorption of small molecules into cross-linked polymer networks is linked to physical properties such as free-volume and cross-link density where the relative penetrability of small molecules is related to their inherent molecular volume (*i.e.* ability to 'fit' into the free volume pores within a polymer network).<sup>11,12</sup> Wiggins and co-workers have demonstrated that manipulation of the average free-volume pore size can be an effective route to preventing solvent ingress into a cross-linked polymeric matrix.<sup>13,14</sup> Small molecule absorption is also influenced by molecular affinity or 'solubility' of the penetrating small molecule within the polymer network.<sup>15</sup> In this case, solvent uptake rate is related to how favourably solvent molecules interact with the host polymer matrix (*e.g.*

<sup>a</sup>Department of Applied Sciences, Northumbria University, Newcastle upon Tyne, NE1 8ST, UK. E-mail: matthew.unthank@northumbria.ac.uk

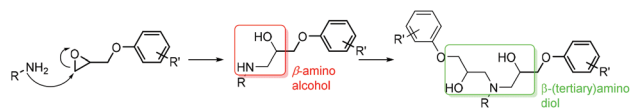
<sup>b</sup>AkzoNobel, Stoneygate Lane, Felling, Gateshead, NE10 0JY, UK

<sup>c</sup>HH Wills Physics Laboratory, Tyndall Avenue, Bristol, BS8 1TL, UK

<sup>d</sup>School of Natural and Environmental Sciences, Bedson Building, Newcastle University, Kings Road, NE1 7RU, UK

†Electronic supplementary information (ESI) available: Experimental procedures, NMR data, IR data, X-ray data, PALS data. CCDC 1894132. For ESI and crystallographic data in CIF or other electronic format see DOI: 10.1039/c9py00780f





**Scheme 1** The formation of  $\beta$ -amino alcohol functionality from the reaction of an amine with an epoxy.

through hydrogen bonding, dipole–dipole interactions or other intermolecular forces) in addition to molecular volume considerations.<sup>16</sup>

This paper describes for the first time a novel hybrid coating material that demonstrates clear performance benefits *vs.* state-of-the-art polymeric materials. Whilst based on established epoxy-amine coating technology, the reported hybrid materials incorporate a new and remarkably chemo-selective reactive transformation during the cure process. Critically, this chemical transformation is achieved without interfering with the primary cure mechanism required to deliver the epoxy-amine thermoset polymer network. This new class of material exploits the selective reactivity of chemical functional groups created during the cure process (Scheme 1). It was hypothesised that exploitation of these functional groups may offer new, unexplored opportunities for controlling transport phenomena of penetrant molecules into coatings, films and membranes. Whilst limited reports exist describing the general use of such functional groups for niche applications,<sup>17</sup> it is true to state that this chemo-selective methodology has not been exploited for direct chemical manipulation in high performance epoxy-amine coatings.

## Experimental

### Materials

The synthesis of epoxy-amine cross-linked polymer networks that are representative of those used in high performance chemical resistant coating, was achieved using the following materials. D.E.N. 431, which is a widely used commercial Novolac epoxy resin, was supplied by Olin Epoxy (formally DOW Chemicals) and is a semi-liquid resin with a number average functionality of 2.8.<sup>18</sup> As a reactive partner/curing agent, 4,4'-methylenedicyclohexanamine (4,4'-MDH) was selected due to its wide commercial use as a curing agent for epoxy resins in coating applications (Fig. 1).

Other materials used in this research programme were all purchased from Sigma Aldrich and used without further purification. These include: phenylglycidyl ether (PGE), cyclohexylamine (CHA), 4-methylcyclohexylamine (MeCHA), 1-methylimidazole (1-MI) and 2-ethyl-4-methylimidazole (2-Et-4-MeI), trimethylborate (TEM), triethylborate (TEB), triisopropylborate (TIB), tributylborate (TBB), methanol, 1,2-dichloroethane (EDC), vinyl acetate (VAM), toluene, acetonitrile, triethylamine, 1,8-diazabicyclo[5.4.0]undec-7-ene (DBU), triazabicyclodecene (TBD), *N,N*-dimethylbenzylamine, and 2,4,6-tris((dimethylamino)methyl)phenol.

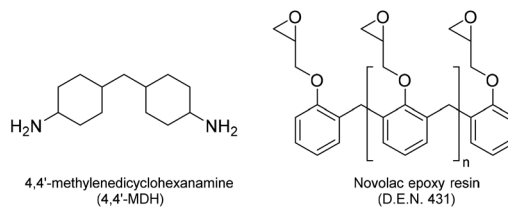


**Fig. 1** The structure of 4,4'-methylenedicyclohexanamine (4,4'-MDH) and Novolac epoxy resin (D.E.N. 431).

### Curing and solvent uptake procedure

D.E.N. 431 (5.0 g, 0.0285 moles of epoxy groups) was thoroughly mixed at room temperature with 4,4'-methylenedicyclohexanamine (1.496 g, 0.0285 moles of N–H groups) and optionally (EAB hybrid materials only) with triethylborate (0.416 g, 0.00285, 10 mol% based on moles of epoxy groups). The mixture was applied using a 400  $\mu$ m cube applicator to the required number of glass microscope slides pre-weighed (g) accurately to 4 decimal places. The coated slides were then placed in an environmental cabinet held at 23 °C and 50% relative humidity and allowed to cure for 24 hours. The hard, coated slides were then placed in a fan assisted oven and held at 80 °C for 16 hours. On removal from the oven, the slides were allowed to cool to room temperature and immediately weighed and the mass recorded (g) to 4 decimal places. Solvent ingress rates and saturated solvent equilibrium concentrations were then measured *via* immersion studies of the cured films in selected solvents over a 28 day period. Each slide was placed in an individual glass jar containing either vinyl acetate ( $\times 3$ ), 1,2-dichloroethane ( $\times 3$ ) and methanol ( $\times 3$ ). These small polar solvent molecules were specially selected as they are known in the chemical transport industry to be the most challenge for transportation,<sup>19</sup> mainly due to high penetration into organic coatings. Three coated slides for each solvent were used. The mass uptake of the solvents was monitored by removing the glass slides periodically from its jar, drying the surface of the coated slide with tissue and immediately weighing the slide to 4 decimal places. The uptake was expressed as a % of the mass of the original film, calculated as follows:

$$\% \text{Uptake} = \frac{\text{Mass immersed slide} - \text{Mass coated slide after cure}}{\text{Mass coated slide after cure} - \text{Mass glass slide}} \times 100\%$$

The results used in this paper represent the average uptake of the three slides for each immersed liquid after 28 days immersion at room temperature. Standard deviations are shown where appropriate.

### Kinetic data by near infra-red spectroscopy

4-Methylcyclohexylamine (2 g, 17.7 mmol) and phenylglycidyl ether (5.31 g, 35.3 mmol) were combined in a glass vial and mixed thoroughly. A portion on this blended mixture was placed in a temperature controlled cell of fixed path length (2.0 mm) in a near infra-red (NIR) spectrometer (PerkinElmer:



Spectrum One instrument) at  $25 \pm 1$  °C. Spectra were run from 5000 to 4000  $\text{cm}^{-1}$ , at constant time intervals and collected automatically using PerkinElmer Time Base v2.0. A blank spectrum was taken before the start of the experiment and subtracted automatically from each succeeding spectrum. The change in peak height of the epoxy peak at 4530  $\text{cm}^{-1}$  was measured relative to the aromatic combination band at 4676  $\text{cm}^{-1}$ . Peak height at 100% conversion was obtained by heating the cell and reaction mixture at 80 °C for 1.5 hours before obtaining the final NIR spectrum.

### Thermal analysis

Differential scanning calorimetry (DSC) was conducted using a PerkinElmer Jade DSC with intercooler and nitrogen supply at a scan rate of 20 °C per minute across a temperature range of -50 °C to +240 °C. Glass transition temperature data was extrapolated from the heat flow profile and quoted as the  $T_g$  mid-point in all cases. Thermogravimetric analysis (TGA) was conducted using a PerkinElmer TGA-7 instrument at a heating rate of 5 °C per minute from 50 °C to 700 °C. The reported onset degradation temperature is defined as the initial inflection point on the weight% scale which precedes the rapid onset of mass loss on further heating.

### Positron annihilation lifetime spectroscopy data

Positron annihilation lifetime spectroscopy (PALS) is, today, a well proven experimental technique as an *in situ* and non-destructive probe for the detection and quantitative evaluation of open volume pores which are often referred to as 'free-volume holes' in polymeric materials. A positron injected into such a medium thermalizes quickly (within a few picoseconds) followed by the formation of a positronium (Ps) almost exclusively within these pores<sup>20</sup> from where they eventually annihilate with lifetimes characteristics of the annihilation sites. A positronium is a hydrogen-like atom consisting of a positron (antiparticle of the electron) and an electron. Depending on the spin configurations of the constituent particles, positronium can either exist in the short lived (vacuum lifetime ~125 ps) *para*-Positronium state (*p*-Ps: anti-parallel positron and electron spins) or in the long lived (vacuum lifetime ~142 ns) *ortho*-Positronium state (*o*-Ps: parallel positron and electron spins). When confined within a pore in matter, the lifetime of the long-lived *o*-Ps (which has a relative abundance of three times that of the *p*-Ps) is drastically reduced (to a few ns). This reduction in lifetime is dictated by the number of collisions of the *o*-Ps with the 'pore-walls', leading to an accurate correlation between the measured *o*-Ps lifetimes,  $\tau_{o\text{-Ps}}$ , to the sizes ( $\nu_h$ ) and size-spread ( $\sigma_h$ ) of the pores (holes) from where they annihilate. The presence of ingressing molecules in close proximity of the pores would also affect the *o*-Ps lifetimes leading to a signature of the pore chemical or physical environments.<sup>21</sup> In the analysis of the lifetime spectra in this study, we have used spectrum fitting procedures to evaluate both discrete lifetimes (which assumes that the *o*-Ps annihilates from an ensemble of 'single size' pores) as well as lifetime distributions (assuming a distribution of a wide range of pore sizes

around a peak; a more realistic scenario for the materials under study here).<sup>22</sup> This analysis mode provides a peak value in the lifetime distribution corresponding to a measure of the average lifetime obtained from the discrete mode,  $\tau_{o\text{-Ps}}$ , together with a lifetime distribution  $\sigma_{o\text{-Ps}}$  which lead to the  $\nu_h$  and  $\sigma_h$  values mentioned above.

We would like to note that low temperature (~e.g. 83 K for Ar as probe) 'gas adsorption porosimetry', the most widely used conventional experimental technique<sup>23,24</sup> for measuring pore size/size distributions used in micro and mesoporous materials (materials with interconnected pores of dimensions >1 nm; pore size  $\gg$  probe size; high pore-volume fraction) would not be appropriate in the materials and pores under study here for a number of reasons. The most pertinent issue is that the dimensions of the 'free volume pores' in this study (with relatively low total pore-volume fraction and ill-defined pore connectivity) are of the same order of magnitude as the probing gas molecules leading to considerable uncertainties in the experimental data, data analysis and their interpretation.

### X-ray crystallography data

Single crystal diffraction data were collected on a Bruker D8 Vantage diffractometer at 150.0(1) K, using micro-focused CuK $\alpha$  radiation with  $\lambda = 1.54178$  Å. Data were collected and reduced using the Apex3 software.<sup>25</sup> An analytical (multi-scan) absorption correction was applied to the data through the program SADABS.<sup>26</sup> The structure was solved and refined using the Olex2<sup>27</sup> interface to the SHELX<sup>28</sup> suite of programs. All non-H atoms were refined anisotropically with H atoms placed using geometric riding constraints and isotropic parameters related to their parent atom. A minor disorder was present in the structure, omitted from the figure for clarity, with final occupancies calculated from freely refined variables. Key crystallographic data are given in Table 1, with full crystallographic information available from the deposition to the Cambridge Crystallographic Data Centre (deposition number CCDC 1894132†).

**Table 1** Selected crystallographic data for compound 6 (see Scheme 2)

Formula	C <sub>26</sub> H <sub>36</sub> B <sub>1</sub> N <sub>1</sub> O <sub>5</sub>
Crystal system	Monoclinic
Space group	<i>P2</i> <sub>1</sub> / <i>c</i>
<i>a</i> (Å)	13.8609(4)
<i>b</i> (Å)	20.1753(6)
<i>c</i> (Å)	8.7717(3)
$\beta$ (°)	94.944(1)
<i>V</i> (Å <sup>3</sup> )	2443.86(13)
<i>Z</i>	4
<i>R</i> ( <i>F</i> , $F^2 > 2\sigma$ )	0.052
<i>R</i> <sub>w</sub> ( $F^2$ , all data)	0.1497

## Results and discussion

### Post-cure network modification

To explore the concept of post cure network modification of epoxy-amine thermoset materials, films based on D.E.N 431



and 4,4'-MDH were prepared due to their established position in the chemical resistance coating market. The initial formulation studied (F1) included co-curing accelerators 1-methylimidazole (1-MI) and 2-ethyl-4-methylimidazole (2-Et-4-MeI) as is standard practice in commercial coating compositions.<sup>29</sup> This benchmark epoxy-amine thermoset material was used to study the influence of trialkylborate esters in the formation of epoxy-amine-borate (EAB) hybrid materials. Of particular interest was the solvent uptake behaviour of the EAB hybrid material in comparison to the epoxy-amine parent system. A homologous series of materials based on trimethyl-, triethyl-, triisopropyl- and tributyl-borate (*i.e.* C1 to C4) were prepared, where the borate esters were incorporated at 5 mol% into the D.E.N 431/4,4'-MDH F1 formulation and cured according to the procedure described above. This resulted in a set of transparent, hard, smooth films for each of the 5 test formulations (parent F1 formulation plus four EAB hybrid materials). The resulting films were immersed for 28 days in VAM and EDC according to the procedure described above (see Experimental section).

The penetrant solvent absorption behaviour was studied over the 28 day period by sampling each of the materials at predetermined intervals in the immersion schedule. The results from the five test materials are illustrated in Fig. 2. It was observed that the EAB hybrid materials significantly outperformed the epoxy-amine parent material in this test. The weight percentage (wt%) increase in the mass of the test samples on immersion in VAM and EDC dropped significantly when trialkylborates were included in the formulation. This is illustrated most clearly when comparing entry 1 (parent) with entries 3 and 4 in Fig. 2. This shows that the use of either triethylborate or triisopropylborate in the synthesis of an EAB hybrid material was highly effective at preventing penetrant solvent ingress into the resulting cross-linked polymer network. In the highest performing example where the EAB hybrid material was created using triethylborate (entry 3, Fig. 2), the saturated solvent equilibrium concentration of VAM and EDC dropped to 50.2% and 36.4% of the original values (entry 1 vs. entry 3). To put these results into context, it should be noted that the parent epoxy-amine control (entry 1, Fig. 2) was itself selected

due to its established excellent performance as a material for chemical resistant coatings. This discovery was considered highly significant for the development of next generation, higher performing chemical resistant coatings and materials.

To further explore and understand this new class of EAB hybrid material, triethylborate was selected for further investigation to understand; (i) how far the solvent uptake behaviour could be improved and; (ii) to elucidate the structure and mechanism of formation for the EAB hybrid materials. New triplicate sets of thermoset polymer films were prepared (F1 formulation) using 0, 5, 10 and 15 mol% of triethylborate, where the mol% was calculated relative to the total moles of epoxide groups in each formulation. Using VAM and EDC as the penetrant solvent molecules, it was found that the solvent uptake of the EAB hybrid material could be decreased further resulting in saturated solvent equilibrium concentrations of 40.6% (VAM) and 26.5% (EDC), compared to the parent epoxy-amine system (Fig. 3, entries 1 vs. 3).

With insight into the chemical resistant performance of EAB hybrid materials in hand, an investigation was conducted to elucidate both the optimal performance and the molecular origin of performance for these new hybrid materials. A simplified epoxy-amine formulation was devised for further study using only epoxy Novolac resin D.E.N 431 and curing agent 4,4'-MDH (F2 formulation). The 2-MI and 2-Et-4-MeI cure accelerators were removed from the study as these materials are known to play multiple roles in the cure process, which will inevitably lead to a less homogeneous, more difficult to characterise polymer network.<sup>30,31</sup> Films were then prepared according to the same procedure and immersed in the test solvents. For this study, methanol was included alongside VAM and EDC, as methanol is one of the most challenging small molecule to exclude from an organic cross-linked epoxy-amine polymer film due to its high polarity and low van der Waals volume.<sup>13</sup> By sampling the weight percent increase of the polymer films (measured in triplicate), greater insight into both the solvent uptake rate and the saturated solvent uptake concentration was predicted.

In Fig. 4, the parent epoxy-amine material (broken lines, F2 formulation) are directly compared to the optimised EAB

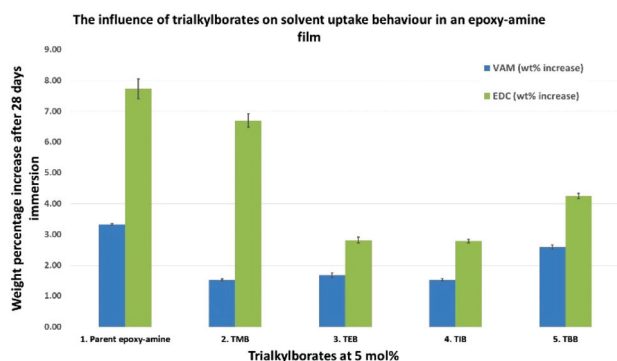


Fig. 2 The reduction in absorption of VAM and EDC through the use of EAB hybrid materials vs. a parent epoxy-amine control.

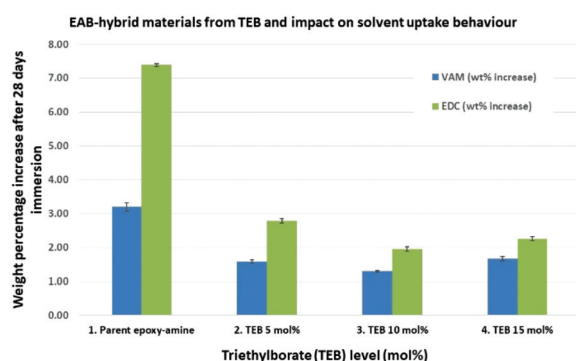


Fig. 3 The relationship between mol% of triethylborate and reduction in solvent uptake in a D.E.N. 431/4,4'-MDH formulation.





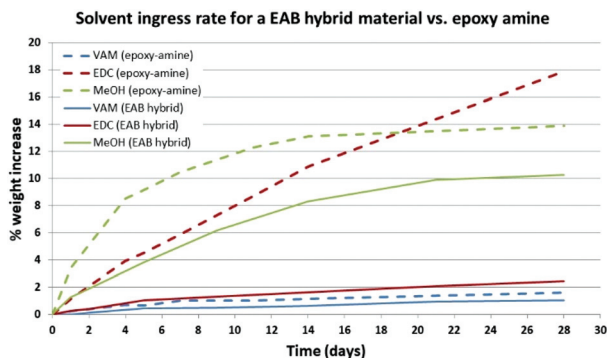


Fig. 4 A comparison of the solvent uptake behaviour of an epoxy amine polymer film based on D.E.N 431 and 4,4'-MDH with 10 mol% triethylborate (solid lines) and without triethylborate (broken lines).

hybrid material (solid lines, 10 mol% triethylborate). The results of this study demonstrate the impressive impact that the incorporation of 10 mol% triethylborate has on small molecule ingress into an epoxy-amine cross-linked polymer network. Most notably, the EAB hybrid material incorporating 10 mole percent triethylborate decreased EDC uptake to 14.0% of its original value (Fig. 4, red lines), whilst at the same time decreasing the most challenging solvent methanol to 74% of its original value (Fig. 4, green lines).

To further test the performance differences between the EAB hybrid material and the parent epoxy-amine control, a repeated absorption-desorption study was conducted using EDC as the test solvent, selected due to its very high uptake in the F2 epoxy-amine parent formulation (Fig. 4, broken line, EDC). This absorption and desorption experiment mimics the 'in-field' conditions experienced in a coated industrial chemical storage or marine shipping transport container, where chemical storage tanks are filled and emptied of their cargoes at regular intervals.

Fig. 5 shows the results of this study and exemplifies the difference in performance between the EAB hybrid material

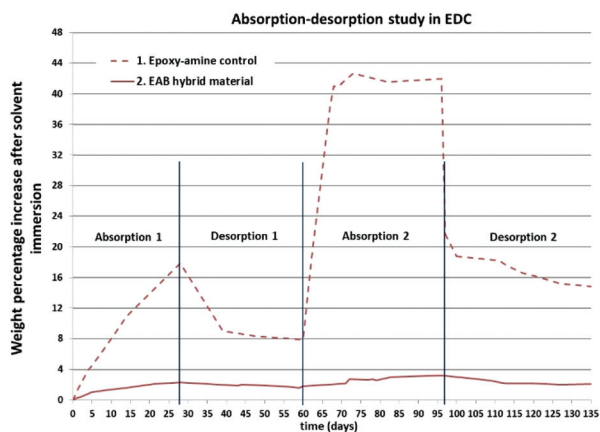


Fig. 5 The absorption-desorption study of parent epoxy-amine control material (entry 1, red broken line) vs. the EAB hybrid material (entry 2, red solid line) in EDC.

and the parent epoxy-amine control. In this experiment, the optimised EAB hybrid material (10 mol% TEB) significantly out performs the epoxy-amine control (F2 formulation) showing a steady and low level absorption throughout the 135 day experiment (Fig. 5, entry 2). In contrast, the parent epoxy-amine control showed an initial 17.9 wt% increase due to EDC ingress on the first absorption cycle, followed by a >40 wt% increase on the second absorption cycle, which also resulted in delamination and degradation of the polymer film, presumably as a result of internal stress build-up within the polymer matrix due to expansion and contraction events.

The impact of this simple modification, achieved through the addition of trialkylborate esters to epoxy-amine thermoset formulations, appears to be highly beneficial in the prevention of low molecular weight polar solvent molecule ingress into the cross-linked polymer network. As previously mentioned, the parent epoxy-amine material was selected for study due to its hugely important role in the coatings industry and in particular, the marine shipping industry. The solvents were selected due to their high level of penetrability in commercial chemical resistant coatings.<sup>19</sup> If deeper understanding into the internal molecular network structure of this new EAB hybrid material could be elucidated, then it was envisaged that there may be far wider reaching implications in the plastics, composite and adhesives industries. To our knowledge, such solvent ingress effects in EAB hybrid materials is unreported in the scientific literature and has now been the subject of two recent patent applications.<sup>32,33</sup>

**Mechanistic investigations.** An investigation was conducted in an attempt to understand the mode-of-action by which the new EAB hybrid materials prevents the ingress of small molecules into epoxy-amine cross-linked polymer networks. Borate esters are known to function as mild Lewis acids due to the presence of a vacant p-orbital on the central boron atom and are therefore capable of coordinating Lewis basic functional groups.<sup>45</sup> It is therefore possible that trialkylborate esters could interact directly with the lone-pair on the epoxide O-atom resulting in acceleration or catalysis of cure.<sup>34</sup> It is also speculated that the inclusion of low viscosity molecules such as trialkylborate esters could delay the onset of vitrification allowing greater conversion of epoxy functional groups into cross-linked junction points within the polymer network.<sup>35,36</sup>

To explore these possibilities, the rate of epoxide ring opening was measured in the presence of a model amine to mimic the role of the 4,4'-MDH curing agent whilst avoiding vitrification which would interfere with the reaction kinetics by limiting diffusion.<sup>35,36</sup> This was studied both with and without triethylborate present in the reaction mixture. Near-infrared spectroscopy was used to monitor epoxide groups consumption according to established literature methods<sup>37-39</sup> (see Experimental section for details).

The experimental results illustrated in Fig. 6 shows the consumption vs. time plot for the reaction of 4-methylcyclohexylamine (MeCHA, the selected model for 4,4'-MDH curing agent) with phenylglycidyl ether (PGE, a model for Novolac resin D.E. N. 431) at 25 °C. The result of this study showed an almost



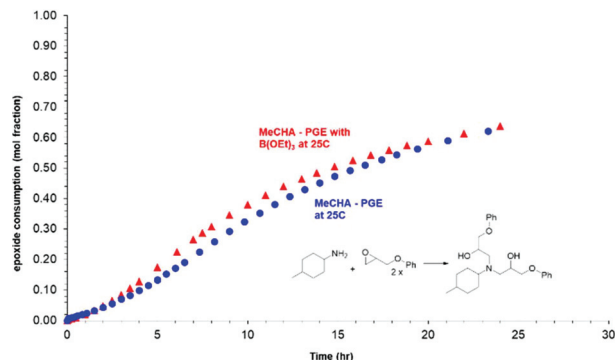


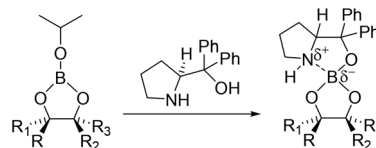
Fig. 6 An illustration of the rate of epoxy-amine reaction vs. time with and without triethylborate.

perfect overlay of epoxy consumption vs. time plots both with (Fig. 6, MeCHA – PGE with  $B(OEt)_3$ , red data points) and without (Fig. 6, MeCHA – PGE, blue data points) triethylborate present in the reactive mixture. This data indicates the absence of any significant acceleration effect from the Lewis acidic triethylborate through Lewis-acid mediated catalysis of the epoxy-amine reaction. Equally, it also indicates the lack of significant complexation of the triethylborate with the Lewis basic amine groups on the MeCHA model curing agent which would result in a deceleration of the reaction rate.<sup>40</sup> Perhaps the latter of these observation is not unexpected given the difference in reported bond energies between the favoured B–O bonds of triethylborate and the proposed B–N bonds.<sup>41–44</sup> Both reaction mixtures showed a slight latent period and ‘S-shaped’ reaction kinetics typical of epoxy-amine reactions and attributed to the known autocatalytic acceleration of this reaction class due to hydrogen bonding from the resulting  $\beta$ -amino alcohols.

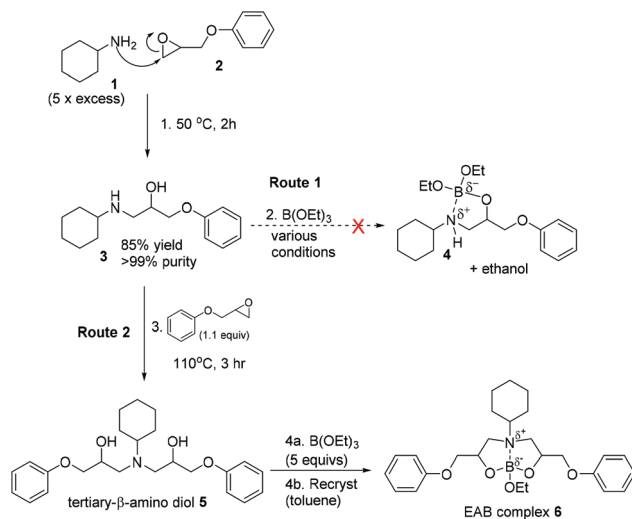
An alternative mechanistic explanation for the formation of EAB hybrid materials can be found in literature reports describing the interaction of trialkylborate esters with  $\beta$ -amino-alcohol functional groups.<sup>45</sup> It is reported that selected  $\beta$ -amino alcohols can react with trialkylborate esters to form borate complexes such as those recently reported by Ortiz-Marciales and co-workers<sup>46</sup> (Scheme 2).

During the cure of epoxy-amine thermoset materials, the ring opening reaction of epoxy groups with amines results in the formation of  $\beta$ -amino-alcohol functional groups. Since we have already established that triethylborate does not interact directly with the epoxide or amine starting materials to any observable extent, the study focussed on understanding whether EAB hybrid materials are formed through complexation of triethylborate with  $\beta$ -amino-alcohol functional groups and at what stage of the cure process this occurs. To explore this hypothesis, cyclohexylamine **1** was reacted in excess with phenylglycidyl ether **2** to give the known<sup>47</sup> model  $\beta$ -amino-alcohol **3** in high purity after crystallisation (Scheme 3, Stage 1).

The isolated  $\beta$ -amino-alcohol **3** was then reacted in a 1 : 1 molar ratio with triethylborate under a range of different conditions in an attempt to form the proposed borate complex



Scheme 2 The reaction of amino-alcohols with alkylborate esters as described by Ortiz-Marciales and co-workers.<sup>46</sup>



Scheme 3 The synthesis of model  $\beta$ -amino-alcohol compounds and complexation experiments with triethylborate.

**4** (Scheme 3, route 1). The study of this reaction by  $^1H$ - and  $^{11}B$ -NMR showed no evidence of the proposed complexation of  $\beta$ -amino-alcohol **3** with triethylborate, with only starting materials isolated at the end of reaction (triethylborate;  $^{11}B$ -NMR = 18 ppm). A range of reaction conditions were studied including tertiary amine catalysis (5 mol%) and increased reaction temperatures in an attempt to drive the formation of the proposed borate complex **4**. Amine catalysts included triethylamine, 1,8-diazabicyclo[5.4.0]undec-7-ene (DBU), triazabicyclodecene (TBD), *N,N*-dimethylbenzylamine, 1-methylimidazole, 2,4,6-tris((dimethylamino)methyl)phenol as well as a catalyst-free control. None of these reaction conditions resulted in the formation of the proposed complex **4**. In a final attempt, the  $\beta$ -amino-alcohol **3** was combined with a large excess (5 molar equivalent) of triethylborate and heated to 90 °C under distillation conditions to remove ethanol as it was evolved *via* the proposed boron-centred transesterification reaction. Sampling of the distillate showed that this contained an azeotropic mixture of ethanol and triethylborate (distillate head temperature 90 °C). The mixture was distilled to dryness and the residue analysed by  $^1H$ - and  $^{11}B$ -NMR. Both the  $^{11}B$ - and  $^1H$ -NMR showed a complex mixture containing multiple chemical species, none of which could be clearly identified as complex **4**. It was concluded that whilst it may be possible to react  $\beta$ -amino-alcohol **3** and triethylborate under forcing conditions, this was not a selective or facile reaction and did not



deliver a product that could be identified as the proposed borate complex **4**. It is hypothesised that the hindered nature of both the cyclohexylamine and the secondary alcohol may render the proposed reaction unfavourable in comparison to the complexes described by Ortiz-Marciales and co-workers.<sup>46</sup> Given the results of this study, it seemed highly unlikely that this was the mode-of-action through which EAB hybrid materials are formed, given the mild cure conditions used in its construction.

As described in Scheme 2, the cure of an epoxy-amine material involves a primary amine functional group (such as those present on curing agents 4,4'-MDH) reacting with an epoxide group on the Novolac epoxy resin. This reaction results in the formation of a secondary- $\beta$ -amino-alcohol functional groups analogous to model compound **3** (Scheme 3, route 1). However, it is well known that whilst the cure temperature ( $T_{\text{cure}}$ ) of curing thermoset remains higher than its glass transition temperature ( $T_{\text{cure}} > T_{\text{g}}$ ) the secondary amines will further react with epoxide groups on the Novolac epoxy resin resulting in the formation of tertiary- $\beta$ -amino diol functional groups. This process is essential for the formation of the required thermoset cross-linked polymer network. To explore the chemistry of trialkylborate esters with this functional group, the tertiary- $\beta$ -amino diol intermediate **5** was prepared. Synthesis was achieved *via*  $\beta$ -amino-alcohol **3** through reaction with a further equivalent of phenylglycidyl ether **2** (Scheme 3, route 2). This model compound is a structural analogue of the tertiary- $\beta$ -amino diol functional groups embedded within a cured epoxy-amine polymer network. It was found that in contrast to secondary- $\beta$ -amino alcohol **3**, the tertiary- $\beta$ -amino diol intermediate **5** reacted immediately and selectively on combination with triethylborate to give the epoxy-amine-borate complex **6** (isolated from toluene by crystallisation). <sup>11</sup>B-NMR analysis of this crystalline material in comparison to triethylborate (*i.e.* the starting material) showed a new single peak at 10.3 ppm and complete consumption of the triethylborate peak at 18 ppm. The ppm shift of this signal is in-line with similar reported *tetra*-coordinate borate complexes based on reactions with amino-alcohols.<sup>46</sup> Evidence for the formation of the proposed complex **6** was supported by <sup>1</sup>H-NMR, however the complex mixture of isomers made absolute structural determination difficult. To demonstrate with confidence that EAB hybrid materials are formed through complexation of tertiary- $\beta$ -amino diol functional groups within the polymer network, crystals of EAB complex **6** were grown in acetonitrile and used to gain absolute structural data *via* single crystal X-ray diffraction experiments. As is illustrated in Fig. 8, the X-ray crystal structure of EAB complex **6** confirmed the structure was indeed as represented in Scheme 3. From this X-ray crystal structure, one can calculate both the length of the three B–O covalent bonds (1.409, 1.451 and 1.465 Å) between the diol functionality of the tertiary- $\beta$ -amino diol and the one remaining ethoxy-group. The longer trans-annular interaction (1.721 Å) between the amine lone-pair (blue) and the vacant p-orbital of the central boron atom (orange) is also clear in this experiment (Fig. 8).

It would appear that the formation of borate complex **6** is entropically favoured in comparison to proposed complex **4**, presumably due to the multi-dentate 'chelate effect' of the tertiary- $\beta$ -amino diol **5**. In-line with this crystal structure determination, stable *tetra*-coordinate adducts of the related boronic acids have precedence in the chemical literature (although outside of the coatings literature) and are also supported by X-ray crystallographic studies,<sup>48</sup> including evidence of the polarised trans-annular B–N bond.<sup>49,50</sup> Reports also confirm that the caged structure resulting from the reaction of multi-dentate amino-alcohol ligands with borate ester are significantly more stable than the parent trialkylborate esters.<sup>51</sup> This research supports the hypothesis that favourable *tetra*-coordinate complexes are formed from the emerging tertiary- $\beta$ -amino diol functional groups embedded within the curing polymer network, resulting in the formation of a new EAB-hybrid material with unique chemical resistance properties (Fig. 7). The experimental evidence described here, strongly supports the hypothesis that triethylborate does not react with the intermediate  $\beta$ -amino alcohol functional groups (*i.e.* analogous to **3**) in the partially cured polymer network, nor does it react with the 4,4'-MDH curing agent (as demonstrated in Fig. 6). Triethylborate therefore exhibits an apparent unique, latent and highly chemo-selective reactivity in the formation of EAB hybrid materials, participating the cure process only in the final stages of reaction. If one imagines that this were not the case, then the primary cure process between the Novolac epoxy resin and the diamine curing agent would be significantly retarded as the intermediate secondary- $\beta$ -amino-alcohol groups (*i.e.* analogous to model compound **3**) would not be available for further cure as a result of borate complexation. This scenario would almost certainly compromise the properties and performance of the resulting thermoset coating, resulting in suppressed cure, decreased glass transition temperature ( $T_{\text{g}}$ ) and increased average free-volume.

To support this hypothesis and to confirm that the primary network structure of the EAB hybrid materials had not been significantly altered, a number of thermal analysis experiments were conducted. The glass transition temperatures ( $T_{\text{g}}$ ) of the epoxy-amine control material and the EAB hybrid material were determined using differential scanning calorimetry (DSC), to determine whether the characteristic reduction in material  $T_{\text{g}}$  with reduced cross-link density could be observed.<sup>52,53</sup> In this experiment the  $T_{\text{g}}$  of the EAB hybrid material (Table 2, entry 2) was measured as 110.1 °C which was slightly higher, but comparable with the parent epoxy-amine control at 108.6 °C. This supports the hypothesis that both materials achieve a similar degree of cure and that vitrification in both cases occurs at the same or similar extent of reaction. This is also supported by the results of the near infrared experiments discussed previously (see Fig. 6). Thermogravimetric analysis of the two test materials showed onset of thermal degradation for both materials to be similar at 338 °C and 344 °C for the epoxy-amine and EAB hybrid materials, respectively. The higher on-set of thermal degradation ( $\Delta T = 6$  °C) is presumably a result of the slightly higher



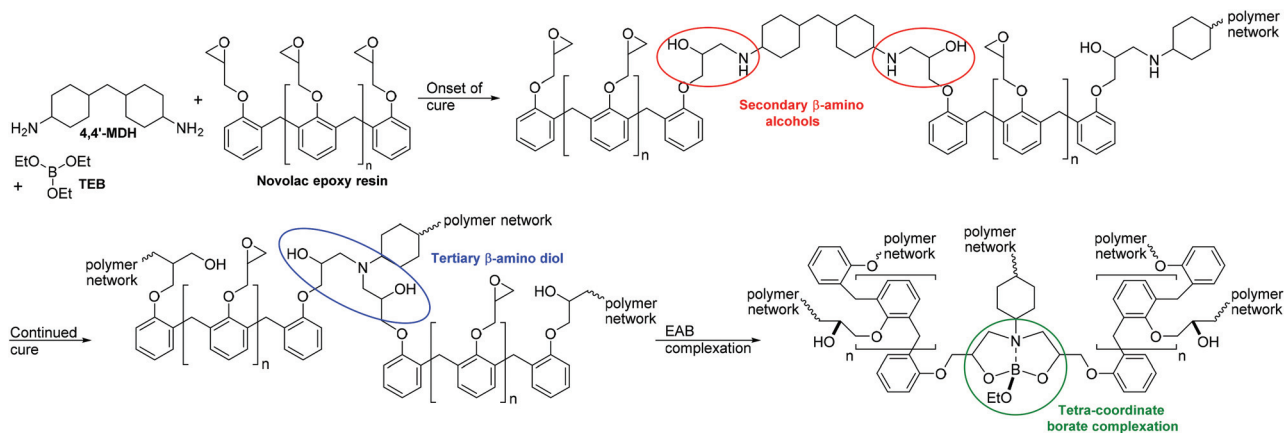


Fig. 7 The proposed formation of  $\beta$ -amino-diol borate complexes *in situ* in a curing epoxy-amine polymer network.

**Table 2** Thermal analysis of epoxy-amine control (entry 1) and epoxy-amine-borate (EAB) hybrid material (entry 2)

Entry	Material	$T_g$ ( $^{\circ}\text{C}$ )	Degradation temp. ( $^{\circ}\text{C}$ )	Residual mass (%)
1	Epoxy-amine	108.6	338	4
2	EAB hybrid	110.1	344	11

measured  $T_g$  of the EAB hybrid material in comparison to the epoxy-amine control. These results confirm the formation of a cross-linked polymer network of high thermal stability and  $T_g$  for both material types. This thermal analysis data supports the hypothesis that the presence of triethylborate in the curing epoxy-amine system does not retard the primary cure process (*i.e.* epoxy-amine cure), allowing formation of the desired cross-linked polymer network *via* a similar time-scale and mechanism, across both material types. The higher residual mass of the EAB hybrid material in comparison to the epoxy-amine control is likely due to the formation of a high thermal stability inorganic boron-oxide structure on thermal decomposition of the organic matter at high temperature ( $>344$   $^{\circ}\text{C}$ ).

This work highlights a novel and potentially unique method for the chemo-selective, post-cure modification of epoxy-amine polymer networks with a clear and beneficial impact on the solvent uptake behaviour, without compromising other critical material properties.

**Positron annihilation lifetime spectroscopy (PALS).** With structural information on the molecular nature of the EAB hybrid materials now in hand, further mechanistic insight was desired to understand why these hybrid materials perform differently to the epoxy-amine parent material. Previous work in the field of positron annihilation lifetime spectroscopy (PALS) has demonstrated a correlation between average free-volume pore (hole) size of a material and the permeability of that material to penetrant solvent molecules.<sup>13</sup> In this work Wiggins and co-workers delivered compelling evidence that epoxy-amine materials with a reduced average free volume pore size prevent the penetration of small molecules more

effectively than those with high average free volume pores.<sup>13,14</sup> To understand whether a reduction in average free volume was responsible for the reduced solvent uptake behavior in EAB hybrid materials, PALS analysis was conducted on the EAB hybrid material and the parent epoxy-amine material respectively. Contrary to expectations, the PALS analysis (Fig. 9) shows that EAB hybrid materials created from triethylborate, 4,4'-MDH and Novolac epoxy resin D.E.N. 431 do not have a lower average free volume pore size in comparison to the parent epoxy-amine material.

Fig. 9 shows that both the average free volume pore size ( $\langle \nu_h \rangle$ ) and size-distribution ( $\sigma_{\nu_h}$ ) in the EAB hybrid material are greater than those of the parent epoxy-amine material at room temperature (21  $^{\circ}\text{C}$  in the positron laboratory). Given the elucidated network structure for the EAB hybrid material described in this paper, it is likely that this increase in average free volume pore size in the EAB hybrid material can be attributed to the loss of intra- and inter-molecular hydrogen bonding between polymer chains within the cross-linked polymer network. The tetra-coordinate complexation of the highly polar tertiary- $\beta$ -amino diol functional groups with trialkylborate ester (as shown in Fig. 7) renders these groups unavailable for hydrogen bonding with other polar functionality within the

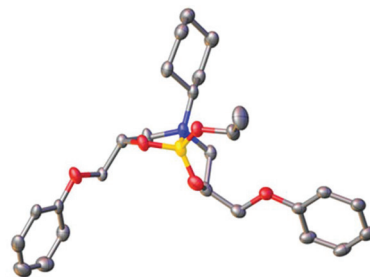


Fig. 8 The chemical structure of the EAB complex 6 as determined by single crystal X-ray diffraction, anisotropic displacement parameters shown at 50% probability with H-atoms and minor structural disorder omitted for clarity.





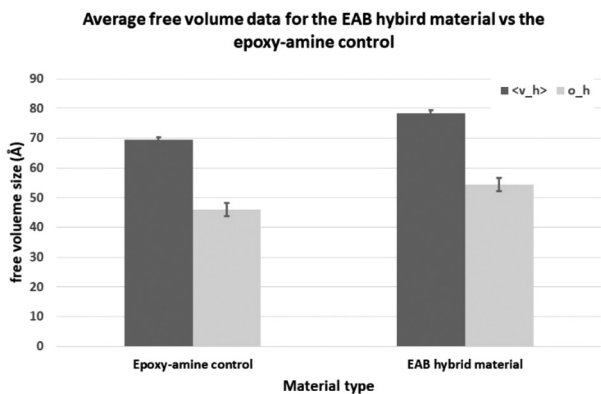


Fig. 9 Free volume hole sizes  $\langle v_h \rangle$  and their distributions,  $\sigma_h$ , for the EAB hybrid material (right) vs. the epoxy-amine control (left) derived from Positron annihilation lifetime spectroscopy (PALS) data.

polymer network. There is a compelling argument that this results in the observed increase in average free volume pore size. By the same argument it is likely that this complexation of polar functionality reduces the affinity of polar penetrant solvents such as VAM, EDC and methanol with the EAB-hybrid polymer network. Given that this type of polar small molecule represents by far the greatest challenge to the developers of chemical resistant coatings, this discovery could be of significant benefit in this field. This evidence offers a good explanation for the origin of reduced solvent ingress/improved chemical resistance of the EAB hybrid materials. What is also clear is that the evidence provided by both the PALS experiments (Fig. 9) and the single crystal X-ray diffraction experiments (Fig. 8) do not support a hypothesis of increased 'secondary' cross-linking as the origin of the EAB hybrid material performance properties.

## Conclusions

In summary, we have reported for the first time, an epoxy-amine-borate (EAB) hybrid material prepared through the network forming reaction of trialkylborate esters, an amine curing agent and a Novolac epoxy resin. Triethylborate has proven to have the ideal chemical reactivity for the post-cure modification of a cross-linked epoxy-amine polymer network, reacting highly selectively with the emerging tertiary- $\beta$ -amino diol functional groups in a latent fashion. It has been demonstrated that this chemo-selective reaction does not interfere with the primary cure mechanism between the epoxy-functional Novolac resin and the amine functional curing agent. Without this high level of chemo-selectivity, the network structure and resulting properties of the epoxy-amine thermoset material would be significantly compromised. Experimental evidence including solvent uptake studies, model reactions, single crystal X-ray diffraction and positron annihilation lifetime spectroscopy, strongly supports the hypothesis that the reduction in solvent ingress in the EAB hybrid materials orig-

inates from the formation of *tetra*-coordinate complexes between the boron atom and the tertiary- $\beta$ -amino diol functional groups that develop within the curing epoxy-amine network. It is proposed that the removal of both H-bond donor (*i.e.* OH groups) and Lewis basic functionality (*i.e.* NR<sub>3</sub> groups) from the polymeric network, reduces the affinity of polar solvent molecules with the EAB hybrid material resulting in an overall reduction in solvent uptake behaviour.

These findings could have potentially wide-ranging applications for the development of high performance materials, composites, plastics and adhesives. This is particularly important in applications where engineering materials, high performance coatings and adhesives are exposed to aggressive chemicals and where it is critical to prevent loss of material integrity and performance. Applications will include Aerospace and Automotive composites, structural adhesives as well as coatings for the global transport and storage of solvents and chemicals. Further work to understand the full scope and potential of this technology is ongoing but it is hoped that this insight into the mode-of-action of these materials will fuel further exploration of chemo-selective post cure modification of thermoset materials.

## Conflicts of interest

There are no conflicts to declare.

## Acknowledgements

The authors would like to thank AkzoNobel for support in this work and for permission to publish this paper. Particular thanks are extended to Dr Alistair Finnie at AkzoNobel his contributions to this publication.

## References

- 1 Epoxy Resin Market report, Grand View Research Inc., Sept 2016.
- 2 Y. J. Weitsman and Y.-J. Guo, *Compos. Sci. Technol.*, 2002, **62**, 889.
- 3 L. W. McKeen, *Permeability Properties of Plastics and Elastomers*, Elsevier Inc., 3rd edn, 2012, pp. 39–58 and 59–75. ISBN: 978-1-4377-3469-0.
- 4 ICIS Chemical Business, 13–19 October 2017, awarded 'Best Product Innovation' for AkzoNobel's Interline 9001 advanced coating system for ship's cargo tanks.
- 5 B. Ellis, *Chemistry and Technology of Epoxy Resins*, Blackie Academic and Professional, 1993, ISBN: 0-7514-0095-5.
- 6 C. May, *Epoxy resins: chemistry and technology*, Marcel Dekker, New York, 2nd edn, 1988.
- 7 M. Sharifi, C. W. Jang, C. F. Abrams and G. R. Palmese, *J. Mater. Chem.*, 2014, **38**, 16071.
- 8 H. Cai, P. Li, G. Sui, Y. Yu, G. Li, X. Yang and S. Ryu, *Thermochim. Acta*, 2008, **473**, 101.



- 9 A. M. Namin, S. Nikafshara and F. Mirmohsenib, *RSC Adv.*, 2015, **5**, 53025.
- 10 S. Morsch, Z. Kefallinou, Y. Liu, S. B. Lyon and S. R. Gibbon, *Polymer*, 2018, **143**, 10.
- 11 N. Ramesh, P. K. Davis, J. M. Zielinski, R. P. Danner and J. L. Duda, *J. Polym. Sci., Part B: Polym. Phys.*, 2011, **49**, 1629.
- 12 J. Sharma, K. Tewari and R. K. Arya, *Prog. Org. Coat.*, 2017, **111**, 83.
- 13 M. Jackson, M. Kaushik, S. Nazarenko, S. Ward, R. Maskell and J. Wiggins, *Polymer*, 2011, **52**, 4528.
- 14 K. Frank, C. Childers, D. Dutta, D. Gidley, M. Jackson, S. Ward, R. Maskell and J. Wiggins, *Polymer*, 2013, **54**, 403.
- 15 B. A. Miller-Chou and J. L. Koenig, *Prog. Polym. Sci.*, 2003, **28**, 1223.
- 16 A. F. M. Barton, *CRC Handbook of Polymer-Liquid Interaction Parameters and Solubility Parameters*, CRC Press, Boca Raton, 1991.
- 17 Q. Shi, K. Yu, X. Kuang, X. Mu, C. K. Dunn, M. L. Dunn, T. Wang and H. J. Qi, *Mater. Horiz.*, 2017, **4**, 598.
- 18 Number average functionality ( $F_n$ ) is defined as the number average molecular weight ( $M_n$ )/epoxy equivalent weight (EEW) of the resin in  $\text{g mol}^{-1}$  (i.e.  $M_n/\text{EEW} = F_n$ ).
- 19 See AkzoNobels Cargo Resistance Guide for information on cargo and sequencing restrictions in the chemical transport sector.
- 20 D. Kilburn, J. Claude, T. Schweizer, A. Alam and J. Ubbink, *Biomacromolecules*, 2005, **6**, 864.
- 21 D. Bamford, G. Dlubek, G. Dommet, S. Horing, T. Lupke, D. Kilburn and M. A. Alam, *Polymer*, 2006, **47**, 3486.
- 22 D. Hughes, C. Tedeschi, B. Leuenberger, M. Roussanova, A. Coveney, R. Richardson, G. Badolato-Bonisch, M. A. Alam and J. Ubbink, *Food Hydrocolloids*, 2016, **58**, 316.
- 23 M. Thommes and K. A. Cychosz, *Adsorption*, 2014, **20**, 233.
- 24 M. Thommes, K. Kaneco, A. V. Neimark, J. P. Olivier, F. Rodriguez-Reinoso, J. Rouquerol and K. S. W. Sing, *Pure Appl. Chem.*, 2015, **87**, 1051.
- 25 APEX3 v2017.3-0, Bruker AXS Inc., 2017.
- 26 SADABS-2016/2, Bruker, 2016.
- 27 O. V. Dolomanov, L. J. Bourhis, R. J. Gildea, J. A. K. Howard and H. Puschmann, *J. Appl. Crystallogr.*, 2009, **42**, 339.
- 28 (a) G. M. Sheldrick, *Acta Crystallogr., Sect. A: Found. Adv.*, 2015, **71**, 3–8; (b) G. M. Sheldrick, *Acta Crystallogr., Sect. A: Found. Crystallogr.*, 2008, **64**, 112.
- 29 V. Jiřová, *J. Appl. Polym. Sci.*, 1987, **34**, 2547.
- 30 F. Ricciardi, W. A. Romanchick and M. M. Joullié, *Polym. Chem.*, 1983, **21**(5), 1475.
- 31 M. S. Heise and G. C. Martin, *J. Polym. Sci., Part C: Polym. Lett.*, 1988, **26**, 153.
- 32 C. Cameron, A. Wright and M. G. Unthank, Coating method for surfaces in chemical installations, WO2015165808, 2015.
- 33 C. Cameron, A. Wright and M. G. Unthank and J. Wood, Coating method for surfaces in chemical installations, WO2017068015, 2017.
- 34 M. T. Sabatini, L. T. Boulton and T. D. Sheppard, *Sci. Adv.*, 2017, **3**(9), 1.
- 35 K. Dusek and I. Havlicek, *Prog. Org. Coat.*, 1993, **22**, 145.
- 36 G. Wisanrakkit and J. K. Gillham, *J. Appl. Polym. Sci.*, 1990, **41**, 2885.
- 37 G. Nikolic, S. Zlatkovic, M. Cakic, S. Cakic, C. Lacnjevac and Z. Rajic, *Sensors*, 2010, **10**, 684–696.
- 38 C. Cameron, M. L. Malthouse, A. R. Marrion, A. C. Wright and M. G. Unthank, Curable thiol-reactive resin coating composition, WO2013107747, 2013.
- 39 L. Li, Q. Wu, S. Li and P. Wu, *Appl. Spectrosc.*, 2008, **62**(10), 1129.
- 40 B. Carboni and L. Monnier, *Tetrahedron*, 1999, **55**, 1197.
- 41 T. L. Cottrell, *The Strengths of Chemical Bonds*, Butterworth, London, 2nd edn, 1958.
- 42 B. de B. Darwent, *National Standard Reference Data Series*, National Bureau of Standards, no. 31, Washington, 1970.
- 43 S. W. Benson, *J. Chem. Educ.*, 1965, **42**(9), 502.
- 44 J. A. Kerr, *Chem. Rev.*, 1966, **66**, 465.
- 45 D. G. Hall, Structure, Properties, and Preparation of Boronic Acid Derivatives. Overview of Their Reactions and Applications, in *Boronic Acids: Preparation and Applications in Organic Synthesis and Medicine*, ed. D. G. Hall, Wiley-VCH Verlag GmbH & Co. KGaA, Weinheim, FRG, 2006.
- 46 V. Stepanenko, M. de Jesus, C. Garcia, C. L. Barnes and M. Ortiz-Marciales, *Tetrahedron Lett.*, 2012, **53**, 910.
- 47 J. R. Lizza and G. Moura-Letts, *Synthesis*, 2017, (6), 1231.
- 48 S. J. Rettig and J. Trotter, *Can. J. Chem.*, 1975, **53**, 1393.
- 49 R. Csuk, N. Muler and H. Sterk, *Z. Naturforsch., B: J. Chem. Sci.*, 1985, **40**, 987.
- 50 T. Mancilla, R. Contreras and B. Wrackmeyer, *J. Organomet. Chem.*, 1986, **307**, 1.
- 51 H. Steinberg and D. L. Hunter, *Ind. Eng. Chem.*, 1957, **49**(2), 174.
- 52 A. R. Kannurpati, K. J. Anderson, J. Anseth and C. N. Bowman, *J. Polym. Sci., Part B: Polym. Phys.*, 1997, **35**(14), 2297.
- 53 R. A. Pearson and A. F. Yee, *J. Mater. Sci.*, 1989, **24**(7), 2571.

